RAPID COMMUNICATIONS

PHYSICAL REVIEW B **80**, 201105(R) (2009)

Switching the electric and magnetic responses in a metamaterial

Xiang Xiong,[1] Wei-Hua Sun,[1] Yong-Jun Bao,[2,1] Ru-Wen Peng,[1,*,†] Mu Wang,[1,*,‡] Cheng Sun,[2,*,§] Xiang Lu,[3] Jun Shao,[3] Zhi-Feng Li,[3] and Nai-Ben Ming[1]

[1]*National Laboratory of Solid State Microstructures and Department of Physics, Nanjing University, Nanjing 210093, China*
[2]*Department of Mechanical Engineering, Northwestern University, Evanston, Illinois 60208-3111, USA*
[3]*National Laboratory for Infrared Physics, Shanghai Institute of Technical Physics, Chinese Academy of Sciences, Shanghai 200083, China*

(Received 29 April 2009; revised manuscript received 20 October 2009; published 20 November 2009)

We demonstrate in this Rapid Communication that in an assembly of stacked metallic U-shaped resonators, pure magnetic and electric responses are, respectively, realized, and the magnetic and electric responses can be switched at the same frequency by changing the polarization of incident light for 90°. This unique feature originates from the topological symmetry of the structure. We suggest that this property opens a gateway to construct metamaterial with tunable permittivity and permeability.

DOI: 10.1103/PhysRevB.80.201105 PACS number(s): 78.20.Ci, 42.25.Ja, 73.20.Mf, 78.67.−n

As an artificial microstructure, metamaterial opens a gateway to achieve electromagnetic properties that are unattainable from natural materials and provides intriguing perspectives for manipulating electromagnetic waves. With deliberately designed metallic microstructures, specific electromagnetic responses occur; hence, artificial magnetism,[1–3] negative refractive index,[4–7] enhanced optical transmission[8–12] and invisible cloaking,[13,14] etc., can be realized. The electric and magnetic responses of a system are usually characterized by permittivity and permeability, which depend not only on the intrinsic structure of the material but also on the polarization of incident light. Yet studies so far concentrate most on finding new geometries to achieve desired electric and magnetic responses, and very few researches have been done on the role of external excitation fields.

Conventional designing of materials with negative refractive index follows the idea to combine a resonant magnetic structure with metal that provides a "background" of negative permittivity in a broad spectral range,[6] including the wavelength where magnetic response occurs.[7,15,16] Yet electric and magnetic components of an electromagnetic wave are coupled. The magnetic response of a metamaterial in fact originates from the interaction of magnetic component of incident light and induced magnetic dipole moment generated by surface electric current.[2] It is intriguing to find out the reasons that electric and magnetic responses are discriminatively excited in these microstructures and to find a way to tailor permittivity and permeability of the structure.

Here, we report that the magnetic and electric resonances of the *same* metallic structure can be switched at the same frequency band by simply altering the polarization of incident light by 90°. This property originates from the constructive/deconstructive superposition of electric and magnetic responses of four orthogonally placed U-shape resonating (USR) elements. Although each individual resonator exhibits distinctive electric and magnetic responses, the collective response of all the resonators in the unit can be purely electric or magnetic. Our finding offers an interesting implication for metamaterial design that one can achieve the bulk properties that fundamentally differ from that of each individual element.

The elementary building block of the metallic structure consists of two types of USR pairs, U_1 and U_2. For U_2 [Fig. 1(a), right], its upper and lower layers have been rotated, respectively, with respect to that of U_1 [Fig. 1(a), left]. Four pairs of such USR elements assemble a unit, where the elements in diagonal direction are identical [Fig. 1(b)]. An array of such units is arranged in a simple square lattice. The coordinate frame is so set that the diagonal directions of USRs are defined as $\boldsymbol{x}$ and $\boldsymbol{y}$ directions, respectively, as shown in Fig. 1(a). Meanwhile, the opening of U_1 on the upper layer points to 45°, while that on the lower layer points to −45°. Light incidents along $+z$ and the polarization (defined as the direction of $\vec{E}$) are characterized by angle θ.

With the finite difference time domain method (CST Mi-

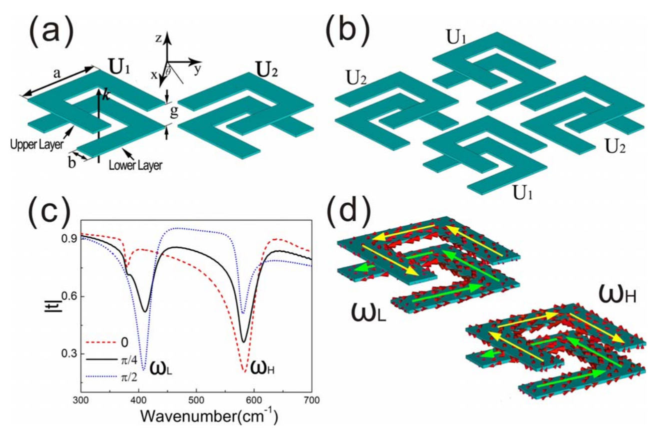

FIG. 1. (Color online) (a) The structure of stacked and orthogonally rotated USR pairs (U_1 and U_2). (b) The unit constructed with U_1 and U_2. The elements in the diagonal directions are identical. (c) Transmission coefficients ($|t|$) with different polarization ($\theta=0$, x polarization; $\theta=\pi/4$; and $\theta=\pi/2$, y polarization). Two resonant dips locate at ω_L and ω_H, respectively. (d) The calculated surface current density excited on USRs at lower and higher resonant frequencies, respectively. The red/gray small arrows represent the calculated local current distribution, and highlighted arrows represent the effective current. In the calculation, both the interlayer and the substrate are set as vacuum, and $\boldsymbol{a}=4.0$ μm, $\boldsymbol{b}=1.0$ μm, and $\boldsymbol{g}=600$ nm.

crowave Studio), we calculate the transmission coefficients of USRs array with different polarization [Fig. 1(c)]. Independent of polarization of incident light, two resonant dips appear around $\omega_L = 400\ \mathrm{cm}^{-1}$ and $\omega_H = 590\ \mathrm{cm}^{-1}$, respectively. Surface current densities on U_1 at these two resonant frequencies are illustrated in Fig. 1(d) with small arrows. The effective-induced electric currents on each layer of USRs are schematically illustrated by the highlighted long arrows. One may find that at ω_L, the electric currents on the upper and lower layers of USRs flow in parallel; whereas at ω_H, the currents on the two layers are antiparallel. The detail surface current analysis and corresponding electric/magnetic field distributions are provided in the supporting material.[17] It should be emphasized that the mode of the induced electric current on a USR pair is independent of the polarization of incident light.

The relative direction of the induced current in elements U_1 and U_2, however, depends on the polarization of incident light. For example, as illustrated in Fig. 2(a), when the normal incident light is $\boldsymbol{x}$ polarized, at ω_L the excited currents on both upper and lower layers of U_1 flow in the same direction and are anticlockwise; meanwhile, those on U_2 flow in the same direction, yet they are clockwise. When the incident light is $\boldsymbol{y}$ polarized, at the same frequency, the excited surface currents on both layers of U_1 and U_2 are anticlockwise, as shown in Fig. 2(b). The induced surface currents on U_1 and U_2 at ω_H have the similar feature and are shown in Fig. 2(c) (for $\boldsymbol{x}$ polarization) and Fig. 2(d) (for $\boldsymbol{y}$ polarization), respectively.

Whether a response is magnetic or electric depends not only on the mode of surface electric currents[18,19] but also on the polarization of the incident light. From Fig. 2, one may easily find that the excited circular currents on USRs generate the induced magnetic fields H'_z, which either cancel out in the unit cell [Figs. 2(a), 2(c), and 2(d)] or is along the propagation direction of incident light [Fig. 2(b)], and does not add to the incident field. So the induced vertical magnetic moments do not contribute to the resonance in permeability μ.[20] However, situation differs in the horizontal plane. To elucidate this, we project the induced surface currents on upper and lower layers of USRs in directions along $\boldsymbol{x}$ axis and $\boldsymbol{y}$ axis, respectively. Let us take element U_1 as an example [Fig. 2(a), left]. At ω_L, the projected currents on the upper and lower layers of U_1 along $\boldsymbol{x}$ direction are antiparallel; whereas those along $\boldsymbol{y}$ direction are parallel. This means that curl integration along the loop in x-z plane is nonzero, indicating an induced magnetic field $\boldsymbol{H}'$ is established according to Ampere's law. Along $\boldsymbol{y}$ direction, in $\boldsymbol{y}$-$\boldsymbol{z}$ plane, two parallel projected currents on the upper and lower layers suggest that there exists an induced electric field $\boldsymbol{E}'$ along $-\boldsymbol{y}$ direction according to Ohm's law. Similar analysis can be applied to U_2 [Fig. 2(a), right], where a magnetic field $\boldsymbol{H}'$ is induced in $+\boldsymbol{y}$ direction, and an electric field $\boldsymbol{E}'$ is induced in $+\boldsymbol{y}$ direction. Therefore, when the incident light is $\boldsymbol{x}$ polarized, by combining U_1 and U_2, as that shown in Fig. 2(a), a pure induced magnetic field is established in $\boldsymbol{y}$ direction, which is in the same direction of the magnetic component of the incident light; the induced electric fields in U_1 and U_2, however, are in the opposite directions, and hence are canceled out [Fig. 2(a)]. Consequently, a pure magnetic response is excited by $\boldsymbol{x}$-polarized light in this scenario.

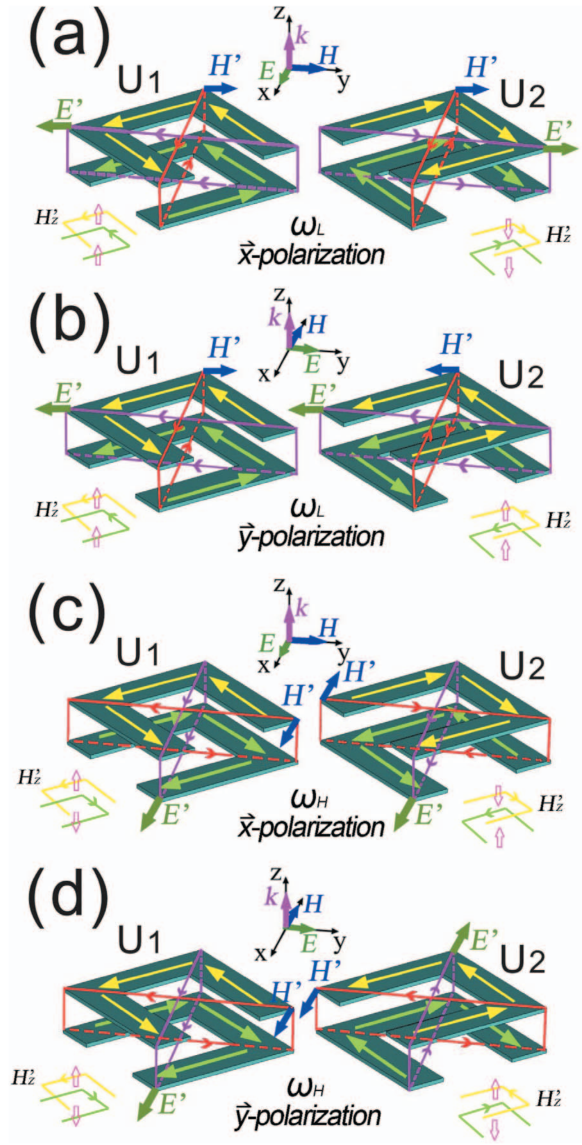

FIG. 2. (Color) By setting $\boldsymbol{x}$ and $\boldsymbol{y}$ axes along the diagonal directions of USRs, we project the induced surface current along $\boldsymbol{x}$ and $\boldsymbol{y}$ directions. (a) for $\boldsymbol{x}$-polarized incident light, at ω_L the induced electric fields contributed by U_1 and U_2 are canceled; whereas the induced magnetic fields sum up and are along the direction of the incident light. In this scenario, magnetic response occurs. (b) for $\boldsymbol{y}$-polarized incident light, at ω_L the induced magnetic fields contributed by U_1 and U_2 are canceled; whereas the induced electric fields sum up and are along the direction of the incident light. In this scenario, electric response occurs. (c) and (d) show the situations at high resonant frequency ω_H, where electric (c) and magnetic (d) responses are induced, respectively. It should be noted that the induced magnetic fields in vertical direction H'_z either cancel out in the unit cell or along the $\boldsymbol{k}$ vector of incident light. They do not add to the incident field $\boldsymbol{H}$.

Each separated element U_1 or U_2 is polarimetric due to chirality of the structure. However, by combining U_1 and U_2 in the way as we show above, a linear response is generated when the polarization of incident light is along the diagonal directions of USRs. The diagonal directions of USRs can be

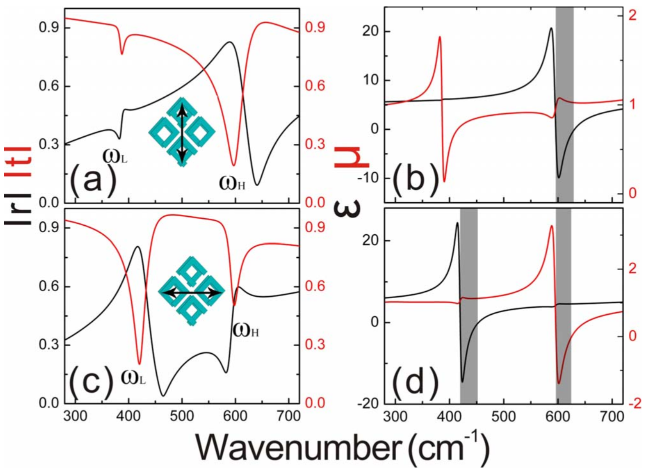

FIG. 3. (Color online) (a) The calculated transmission ($|t|$) and reflection ($|r|$) coefficients for $\boldsymbol{x}$-polarized incident light. (b) The retrieved permittivity and permeability with $\boldsymbol{x}$-polarized incident light. (c) The calculated transmission ($|t|$) and reflection ($|r|$) coefficients for $\boldsymbol{y}$-polarized incident light. (d) The retrieved permittivity and permeability with $\boldsymbol{y}$-polarized incident light. The shaded regions denote the zones with negative effective permittivity and permeability, respectively.

considered as the principal axes of this metamaterial. The topological symmetry of the structure is responsible for the unique features presented here.

Similarly, for $\boldsymbol{y}$-polarized incident light, at ω_L, induced magnetic field is along $+\boldsymbol{y}$ direction and induced electric field in $-\boldsymbol{y}$ direction on U_1 [Fig. 2(b), left]; on U_2, both induced magnetic and electric fields are in $-\boldsymbol{y}$ direction [Fig. 2(b), right]. So, by combining U_1 and U_2, as shown in Fig. 2(b), induced magnetic fields along $\boldsymbol{y}$ direction are canceled out, whereas a purely induced electric field is established along $-\boldsymbol{y}$ direction, which is exactly in the same direction of the electric component of incident light. Therefore, a purely electric response is excited [Fig. 2(b)].

The same analysis can be applied at ω_H. It turns out that with the combination of U_1 and U_2, electric response can be established when incident light is $\boldsymbol{x}$ polarized [Fig. 2(c)], and magnetic response is established when the incident light is $\boldsymbol{y}$ polarized [Fig. 2(d)]. We therefore conclude that both $\boldsymbol{x}$-polarized and $\boldsymbol{y}$-polarized incident lights can equivalently excite either electric or magnetic response.

The unit consisting of elements U_1 and U_2 in the way shown in Fig. 1(b) is applied as the building block to construct an array with a simple square lattice. The transmission and reflection coefficients of the array are shown in Figs. 3(a) and 3(c) for $\boldsymbol{x}$- and $\boldsymbol{y}$-polarized incident lights, respectively. In both cases, two resonances appear, respectively, at ω_L and ω_H. Calculation indicates that for both scenarios, there is no change in polarization orientation, so the retrieval method based on S parameters[21] can be safely applied. Figures 3(b) and 3(d) illustrate the effective permittivity ε_{eff} and effective permeability μ_{eff} of the structure. Magnetic response occurs at ω_L when the incident light is $\boldsymbol{x}$ polarized (characterized by an evident jump in μ_{eff}); electric response occurs at ω_H (characterized by an evident jump in ε_{eff}) for the same polarization. For $\boldsymbol{y}$-polarized incident light, electric response occurs at ω_L and magnetic response occurs at ω_H, instead. This means that $\boldsymbol{x}$ and $\boldsymbol{y}$ axes are indeed the principal optical axes of the structure, along which purely electric/magnetic responses to external excitation are achieved. By changing the polarization of incident light for 90°, magnetic and electric responses of the system can be switched at the same frequency.

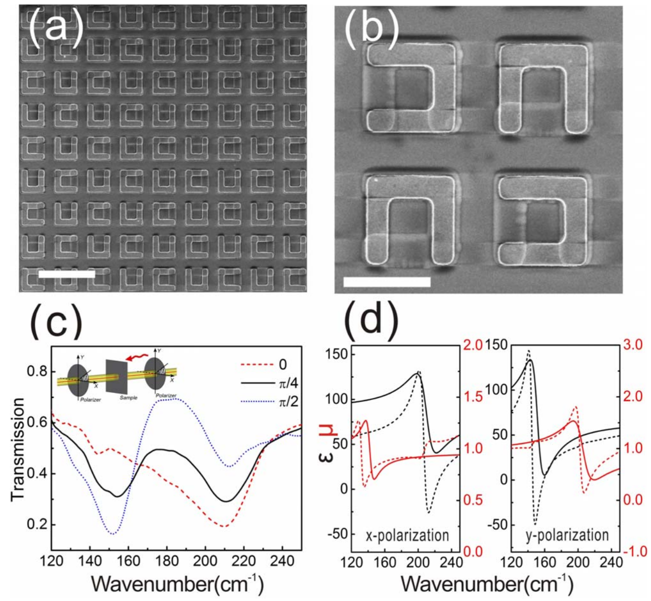

FIG. 4. (Color online) (a) Scanning electron micrograph of USR array fabricated by the alignment nesting lithography. The bar stands for 10 μm. (b) The detail micrograph of the unit of USRs. The arms of lower layer USRs look wider than that on the upper layer due to the coverage of Si_3N_4. The bar stands for 4 μm. (c) Experimentally measured transmission spectra with different polarization. The inset shows the schematics of measurement setup. Two resonance dips can be identified. (d) Retrieved permittivity (black solid line) and permeability (red/gray solid lines) from the experimental data with different polarizations. The dashed lines are from the simulation, which act as the guide for the eyes.

Such metallic structure has been fabricated with lift-off process and alignment nesting lithography on a double-polished silicon wafer and details are provided in the supporting material.[17] The USRs are fabricated from gold film 100 nm in thickness, and the first and the second layers of U-shaped patterns are separated by a 600-nm-thick silicon nitride. With alignment nesting lithography, USR in the second layer locates exactly above that the one on the first layer, yet the orientation has being rotated 90° in a specific way. Hence, an array of deliberately arranged array of elements U_1 and U_2 is fabricated [Figs. 4(a) and 4(b)]. Figure 4(c) shows the measured transmission spectra with different polarization (from $\theta=0$ for $\boldsymbol{x}$ polarization to $\theta=\pi/2$ for $\boldsymbol{y}$ polarization). Two resonant dips (ω_L and ω_H) can be identified and their relative strength is polarization dependent, which are consistent with calculations. Experiments also show that polarization property does not change when the incident light is $\boldsymbol{x}$ or $\boldsymbol{y}$ polarized. Figure 4(d) illustrates permittivity and permeability of the metallic structure retrieved from the measured $\boldsymbol{x}$- and $\boldsymbol{y}$-polarized transmission spectra following the method reported in Ref. 22. The retrieval is based on the transmission intensity measurements and the details are provided in the supporting material.[17] For $\boldsymbol{x}$-polarized incident light, the evident drop of ε_{eff} (electric response) occurs at $\boldsymbol{\omega_H}$, and the drop of μ_{eff} (magnetic response) occurs at $\boldsymbol{\omega_L}$. For $\boldsymbol{y}$-polarized incident light, the evident drop of ε_{eff} and μ_{eff} can be identified at $\boldsymbol{\omega_L}$ (electric response) and at $\boldsymbol{\omega_H}$ (magnetic response), respectively. With these data, we confirm that at the same resonant frequency, magnetic and electric responses of the structure can indeed be switched by merely changing the polarization of incident light orthogonally.

In fact, the polarimetric effect of USRs is an interesting topic. A linearly polarized light is shown to change its polarization after passing through an array of split ring resonators and all types of polarization are accessible from the structure.[23] Similar feature indeed exists in an array of U_1 or U_2. However, by setting principal axis as the diagonal directions of USRs, two eigenstates of surface-plasmon resonance appear. Consequently, purely electric and magnetic resonances can be realized and switched by orthogonally changing either the polarization of incident light or the orientation of the metallic structure. If the polarization of incident light deviates from principal axes, an assembly of the eigenstates emerges and hybrid resonances are obtained.

So far the electromagnetic response of USRs has been extensively studied, and the magnetoinductive and electroinductive coupling of the structures has also been investigated.[23–25] What we report here is a feature that the magnetic and electric resonances of the *same* metallic structure can be switched at the same frequency by simply altering the polarization of incident light by 90°. Such a property originates from the constructive/deconstructive superposition of electric and magnetic responses of the USR elements. Although each individual resonator exhibits distinctive electric and magnetic responses, the collective response of the four resonators in a unit can be purely electric or magnetic. This feature reveals a possibility to tailor permittivity and permeability of an artificial microstructure and to construct functional metamaterials.

Authors appreciate the discussions with Xiang Zhang. This work was supported by MOST of China (Grants No. 2004CB619005 and No. 2006CB921804), NSF of China (Grants No. 10625417 and No. 10874068), and Jiangsu Province (Grant No. BK2008012).

*Author to whom correspondence should be addressed.
†rwpeng@nju.edu.cn
‡muwang@nju.edu.cn
§c-sun@northwestern.edu

[1] J. B. Pendry, A. J. Holden, D. J. Robbins, and W. J. Stewart, IEEE Trans. Microwave Theory Tech. **47**, 2075 (1999).
[2] T. J. Yen, W. J. Padilla, N. Fang, D. C. Vier, D. R. Smith, J. B. Pendry, D. N. Basov, and X. Zhang, Science **303**, 1494 (2004).
[3] S. Linden, C. Enkrich, M. Wegener, J. Zhou, T. Koschny, and C. M. Soukoulis, Science **306**, 1351 (2004).
[4] J. B. Pendry, Phys. Rev. Lett. **85**, 3966 (2000).
[5] R. A. Shelby, D. R. Smith, and S. Schultz, Science **292**, 77 (2001).
[6] See, for example, V. M. Shalaev, Nat. Photonics **1**, 41 (2007).
[7] S. Zhang, W. J. Fan, N. C. Panoiu, K. J. Malloy, R. M. Osgood, and S. R. J. Brueck, Phys. Rev. Lett. **95**, 137404 (2005).
[8] T. W. Ebbesen, H. J. Lezec, H. F. Ghaemi, T. Thio, and P. A. Wolff, Nature (London) **391**, 667 (1998).
[9] W. L. Barnes, A. Dereux, and T. W. Ebbesen, Nature (London) **424**, 824 (2003).
[10] Y. J. Bao, R. W. Peng, D. J. Shu, Mu Wang, X. Lu, J. Shao, W. Lu, and N. B. Ming, Phys. Rev. Lett. **101**, 087401 (2008).
[11] W. Wen, L. Zhou, J. Li, W. Ge, C. T. Chan, and P. Sheng, Phys. Rev. Lett. **89**, 223901 (2002).
[12] Z. H. Tang, R. W. Peng, Z. Wang, X. Wu, Y. J. Bao, Q. J. Wang, Z. J. Zhang, W. H. Sun, and Mu Wang, Phys. Rev. B **76**, 195405 (2007).
[13] J. B. Pendry, D. Schurig, and D. R. Smith, Science **312**, 1780 (2006).
[14] R. Liu, C. Ji, J. J. Mock, J. Y. Chin, T. J. Cui, and D. R. Smith, Science **323**, 366 (2009).
[15] U. K. Chettiar, A. V. Kildishev, H. K. Yuan, W. Cai, S. Xiao, V. P. Drachev, and V. M. Shalaev, Opt. Lett. **32**, 1671 (2007).
[16] G. Dolling, M. Wegener, C. M. Soukoulis, and S. Linden, Opt. Lett. **32**, 53 (2007).
[17] See EPAPS Document No. E-PRBMDO-80-R26944 for details about the sample fabrication with microlithography, the retrieval process based on the transmission intensity measurements, surface current analysis and corresponding electric/magnetic field distributions. For more information on EPAPS, see http://www.aip.org/pubservs/epaps.html.
[18] Y. Liu, N. Fang, D. Wu, C. Sun, and X. Zhang, Appl. Phys. A: Mater. Sci. Process. **87**, 171 (2007).
[19] A. N. Grigorenko, A. K. Geim, H. F. Gleeson, Y. Zhang, A. A. Firsov, I. Y. Khrushchev, and J. Petrovic, Nature (London) **438**, 335 (2005).
[20] T. F. Gundogdu, I. Tsiapa, A. Kostopoulos, G. Konstantinidis, N. Katsarakis, R. S. Penciu, M. Kafesaki, E. N. Economou, Th. Koschny, and C. M. Soukoulis, Appl. Phys. Lett. **89**, 084103 (2006).
[21] D. R. Smith, D. C. Vier, T. Koschny, and C. M. Soukoulis, Phys. Rev. E **71**, 036617 (2005).
[22] T. Driscoll, D. N. Basov, W. J. Padilla, J. J. Mock, and D. R. Smith, Phys. Rev. B **75**, 115114 (2007).
[23] H. Liu, D. A. Genov, D. M. Wu, Y. M. Liu, Z. W. Liu, C. Sun, S. N. Zhu, and X. Zhang, Phys. Rev. B **76**, 073101 (2007).
[24] C. Enkrich, M. Wegener, S. Linden, S. Burger, L. Zschiedrich, F. Schmidt, J. F. Zhou, Th. Koschny, and C. M. Soukoulis, Phys. Rev. Lett. **95**, 203901 (2005).
[25] N. Liu, H. Liu, S. Zhu, and H. Giessen, Nat. Photonics **3**, 157 (2009).